

Catalytic hydroconversion of pyrolytic bio-oil : understanding and limiting macromolecules formation

M. Ozagac^a, C. Bertino-Ghera^a, D. Uzio^a, A. Quignard^a, D. Laurenti^{b,*}, C. Geantet^b

^aIFP Energies Nouvelles, Rond-point de l'échangeur de Solaize, BP3, 69360 Solaize, France

^bIRCELYON, UMR5256 CNRS-UCBL, 2 avenue A. Einstein, 69626 Villeurbanne cedex, France

*Corresponding author: dorothee.laurenti@ircelyon.univ-lyon1.fr

Supporting information

This document provides additional information on the experimental methodology (section 2) and results (section 3). Additionally to the two studies discussed along the manuscript, we decided to report (paragraph 3.3. of this document) the effect of the catalyst and the gas phase composition on the macromolecules production.

2. Experimental Section

2.1. Experimental set-up

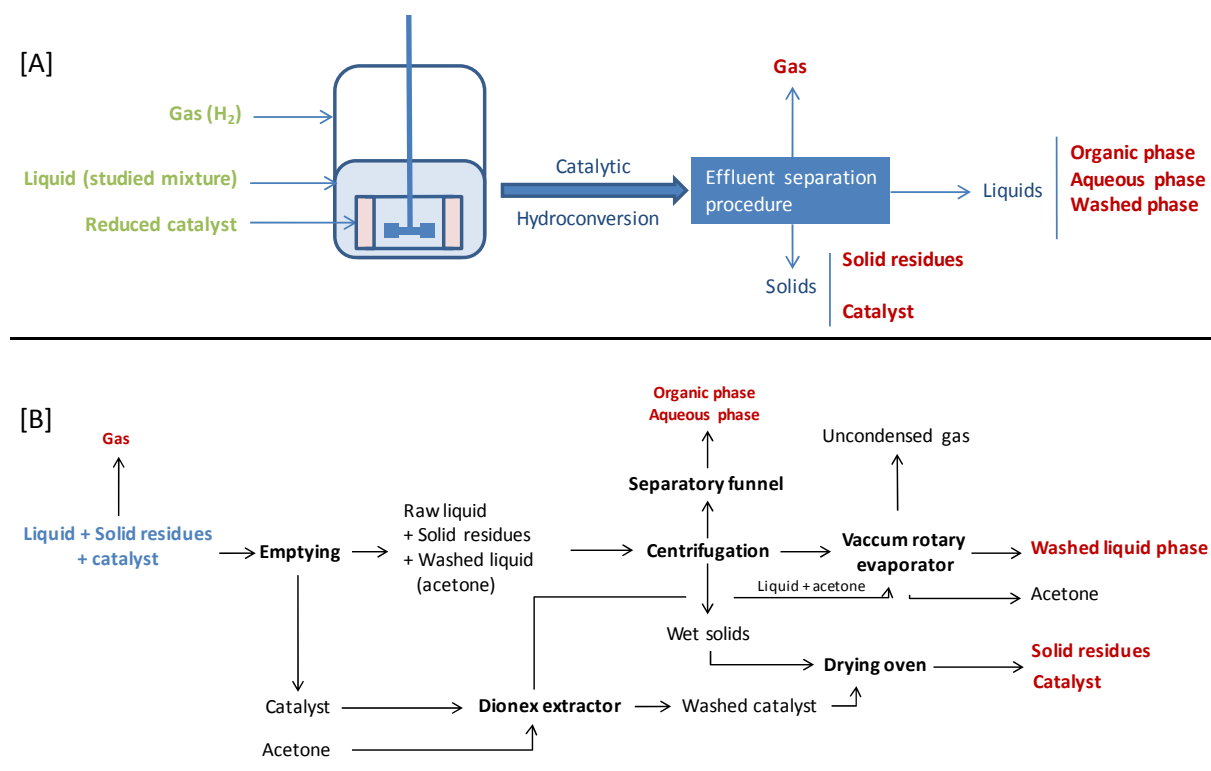


Figure S1. Schematized experimental procedure [A] global [B] detailed

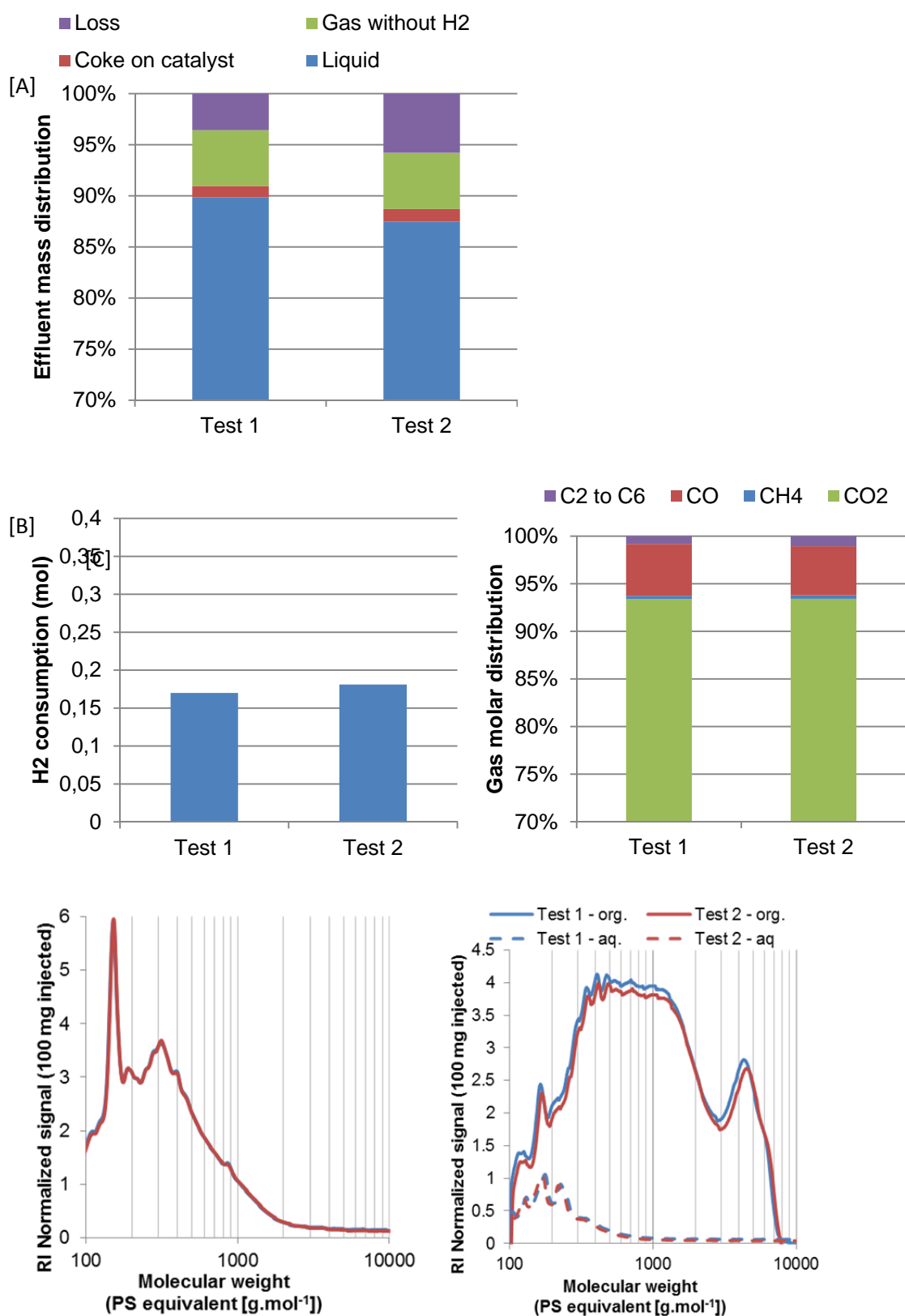


Figure S2. Repeatability tests of the BO catalytic hydroconversion at 250°C during 1 h. [A] Mass distributions, [B] Hydrogen consumption, [C] Gas production, [D] SEC-RI analysis of the introduced BO, [E] SEC-RI analysis of the organic and aqueous effluents

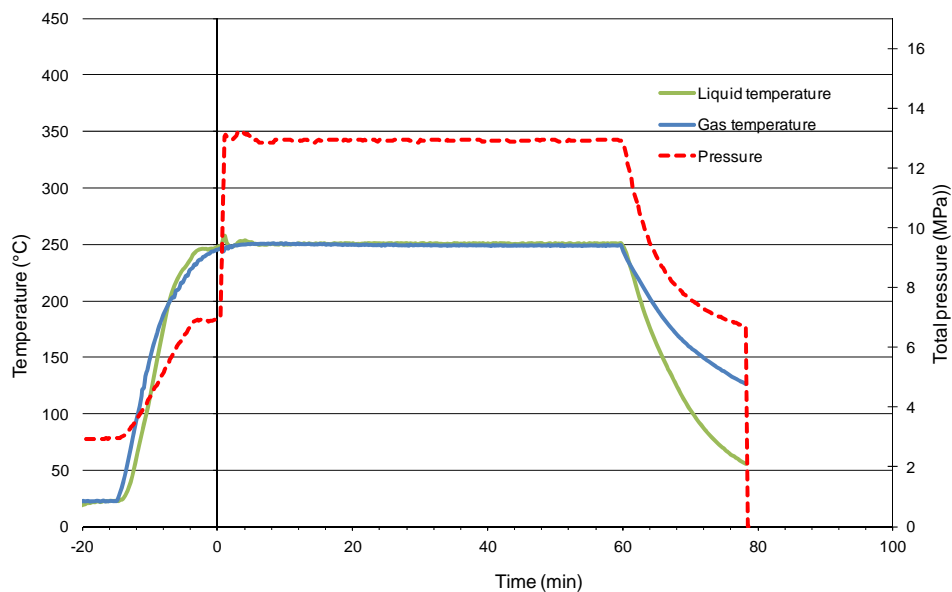
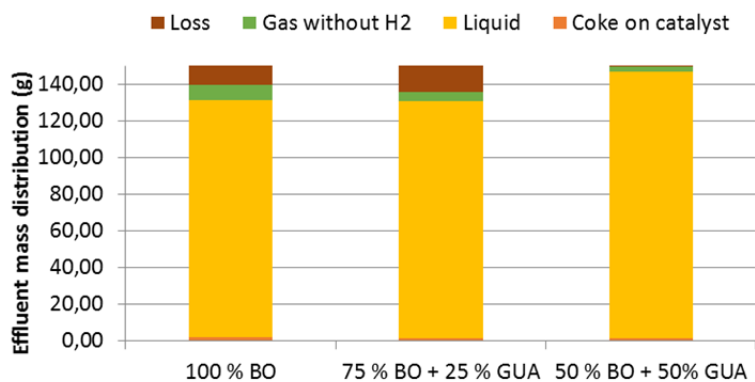


Figure S3. Typical pressure and temperature profiles: catalytic hydroconversion at 250°C during 1 h with a total pressure of 13.0 MPa

2.2. Effect of guaiacol content in BO HDT

We carried out experiments with 25 wt% guaiacol; the conclusions were:

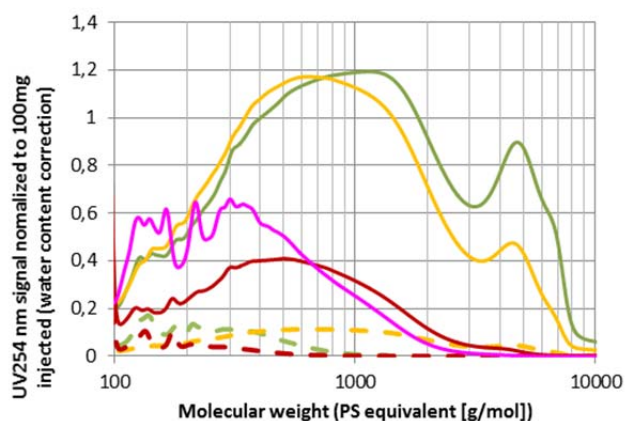
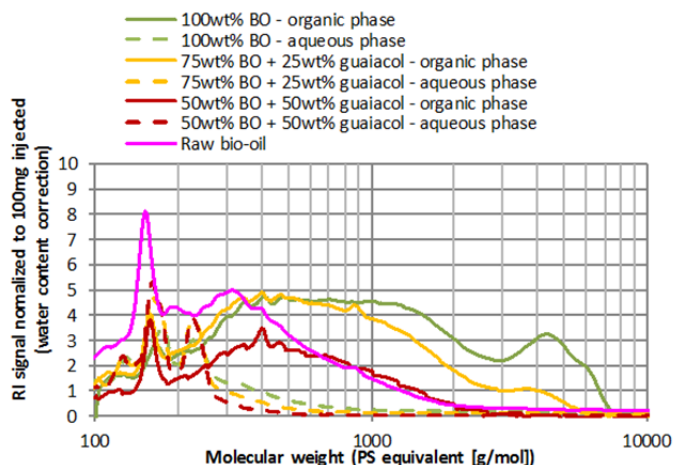
- Extensive losses during the separation due to the viscosity of the mixture and systematic spread of liquid onto the unit piping. That evolved an increase of the experimental mass losses.



W (g)	100 % BO	75 % BO + 25 % GUA	50 % BO + 50% GUA
Coke on catalyst	1,86	1,42	1,58
Liquid	129,50	129,36	145,57
Gas without H ₂	8,27	5,44	2,85
Loss	10,69	14,04	0,52

Figure S4: Experimental fractions mass distribution from HDT of BO and BO/GUA at 250°C during 1 h

- Decrease of formed macromolecules compared to the BO HDT



[A]

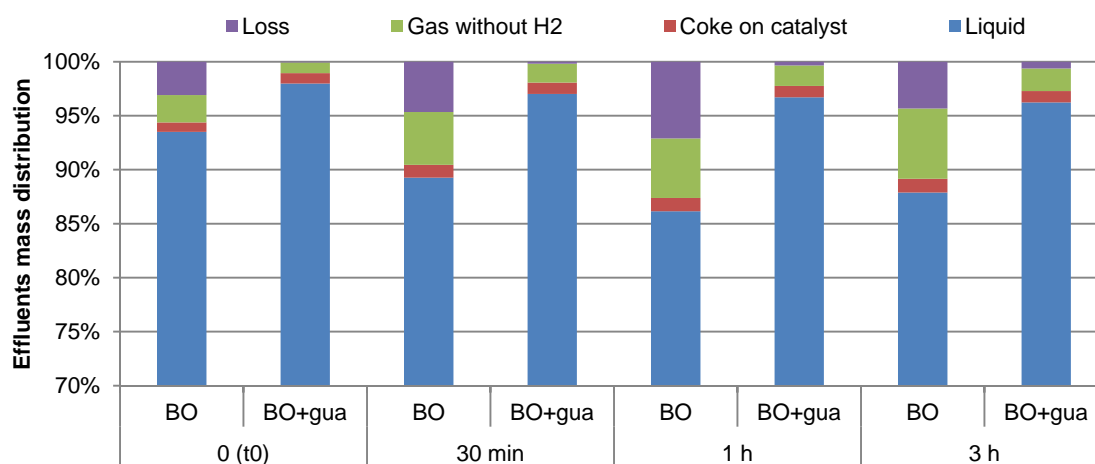
[B]

Figure S5: Normalized SEC analyses of hydroconverted BO and BO+GUA as a function of BO/GUA (1h – 250°C). Continuous line: organic phase; dotted line: aqueous phase [A] RI detection, [B] UV-254 nm detection.

Considering the number of required experimental tests for a BO/GUA 75/25 wt% mixture, we decided to focus our approach with 50:50 ratio.

3. Results and Discussion

3.1. Effect of the reaction time on the bio-oil and bio-oil/guaiacol catalytic hydroconversion



		0 (t0)		30 min		1 h		3 h	
		BO	BO+gua	BO	BO+gua	BO	BO+gua	BO	BO+gua
Mass balance (g)	Liquid	140.4	147.3	134.2	145.9	129.5	145.6	132.2	145.0
	Coke on catalyst	1.3	1.5	1.8	1.6	1.9	1.6	1.9	1.6
	Gas without H ₂	3.8	1.5	7.4	2.6	8.3	2.8	9.8	3.1
	Loss	4.6	0.1	7.0	0.3	10.7	0.5	6.5	0.9

Figure S6. Mass balances from hydroconverted BO and BO+GUA as a function of time (reaction temperature – 250°C)

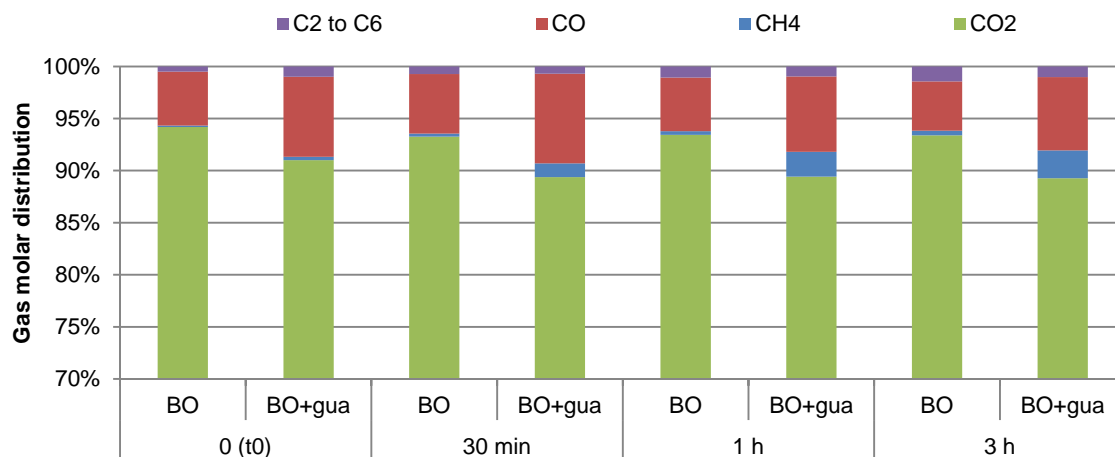


Figure S7. Gas production from hydroconverted BO and BO+GUA as a function of time (reaction temperature – 250°C)

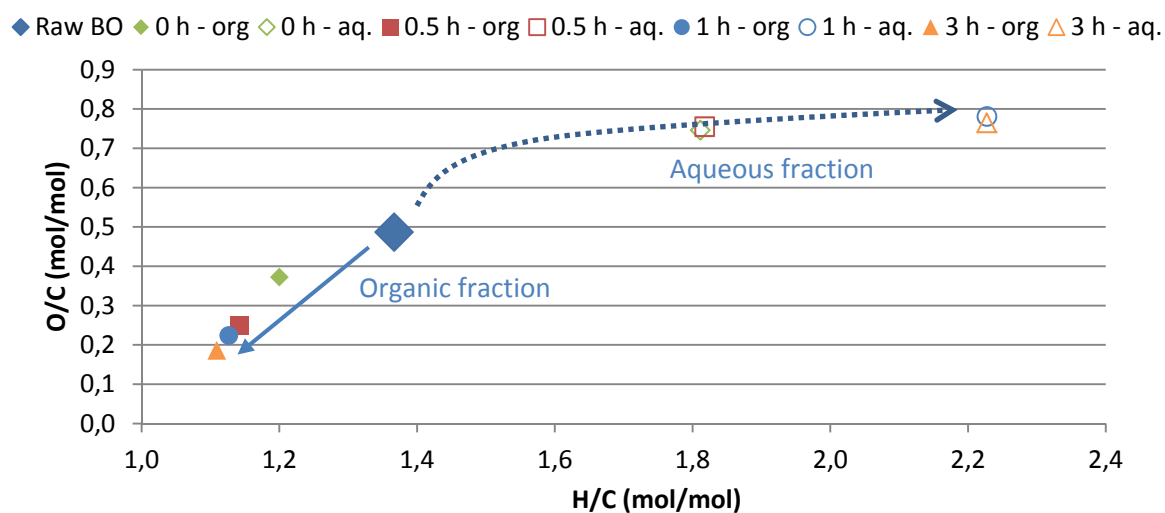


Figure S8. Van Krevelen diagram (Dry basis) reporting the organic “org.” and aqueous “aq.” phases from the hydroconversion of BO as a function of time (reaction temperature – 250°C).

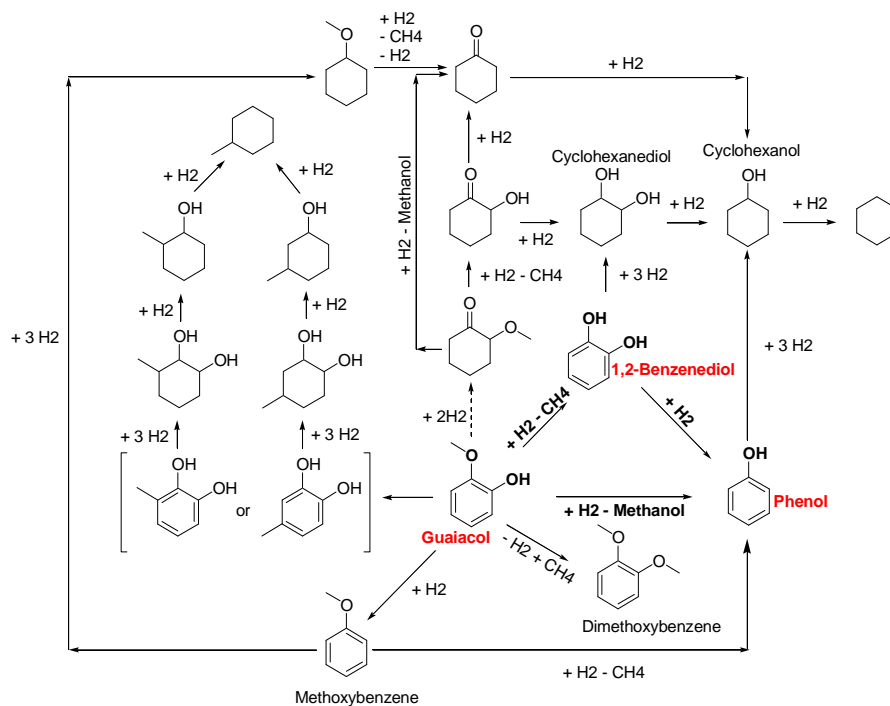


Figure S9. Guaiacol catalytic hydroconversion reaction pathways from GC-FID analysis^[31]

3.2. Comparison of guaiacol effect with some other molecules/solvents:

Six solvents were chosen to better understand the interactions (chemical reaction and/or physical dilution) with bio-oil and its macromolecule precursors. From the studied guaiacol, we chose phenol, anisole and 1,2-benzenediol to identify the potential chemical functions that would be involved in macromolecules precursor conversion while keeping the aromatic ring. Hydroxyl group was studied also with 1-heptanol. Tetralin was chosen to understand the dilution effect of bio-oil without chemical reaction due to oxygenated function. The experimental procedure was respected with 50 wt% of organic solvents reacting at 250°C during 1 h in catalytic hydroconversion conditions. Figure S10 gathers some preliminary results.

SEC analysis presented various signal shapes suggesting different chemical reaction pathways. Contrary to BO+GUA conversion, tetralin did not limit the macromolecules production since the maximal RI signal was beyond 2,000 g.mol⁻¹. The effect of anisole, phenol and heptanol were quite similar with a low conversion (without GC-quantified products) and a maximal macromolecule molecular weight limited to 2,000 g.mol⁻¹. Thus, hydroxyl groups and/or guaiacol-like molecules were prone to react with the macromolecules precursors and limited their extension. 1,2-benzenediol was the most converted product, nevertheless, contrary to guaiacol, no HDO conversion products (such as phenol or benzene) were quantified by GC. The macromolecule limitation and the conversion yield confirm the role of those compounds not only as diluting solvent but also as reactive compounds converting precursors as guaiacol.

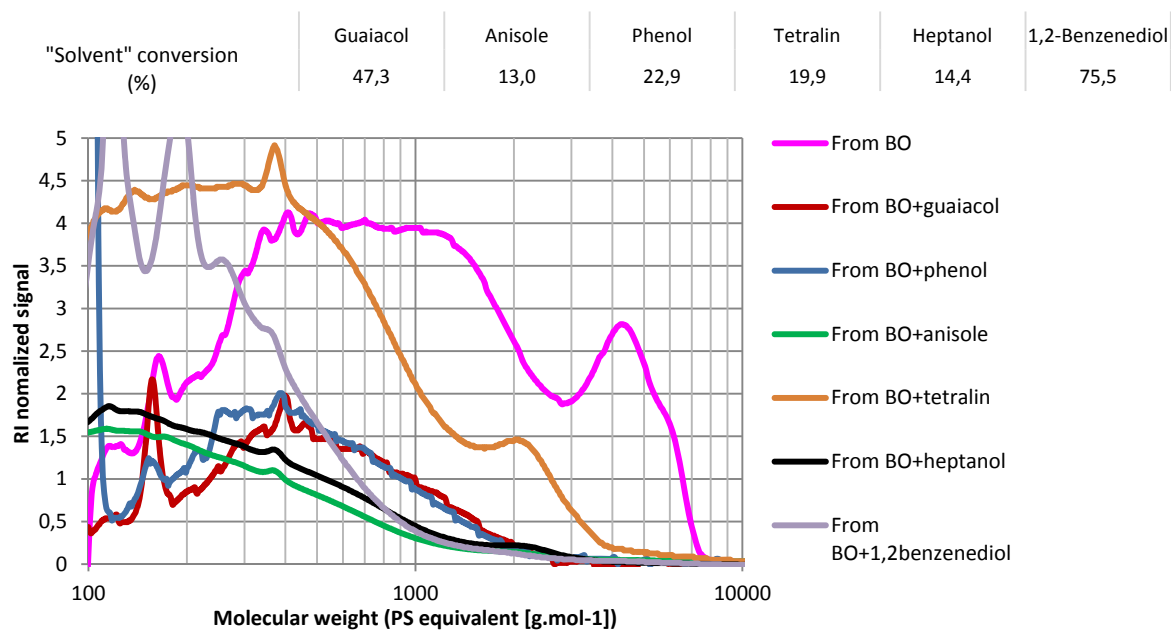


Figure S10. Solvent conversion and normalized SEC analyses from hydroconverted BO and BO+solvents introduced at 50 wt% (1 h – 250°C)

3.3 Characterizations of catalysts

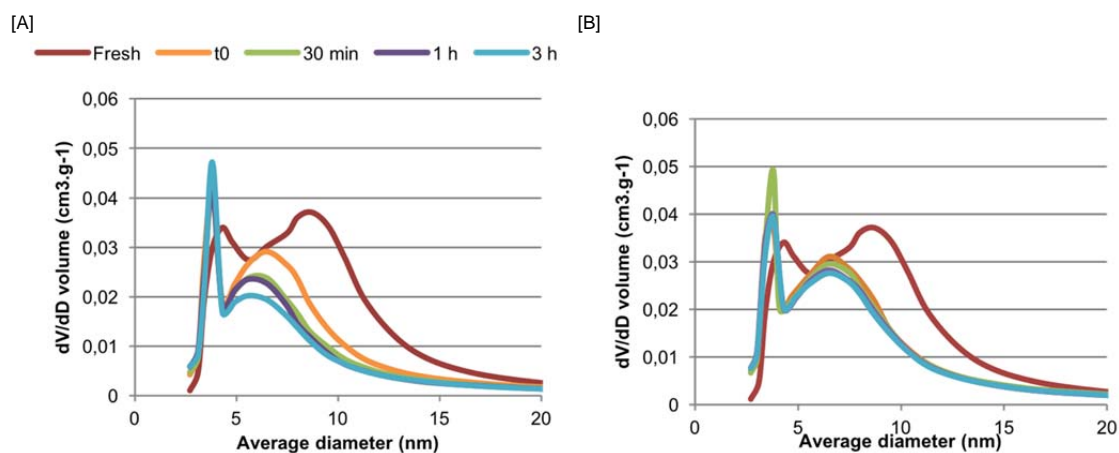


Figure S11. Fresh and used catalysts from BO and BO+GUA hydroconversion as a function of time (reaction temperature – 250°C). Porous distribution from [A] BO, [B] BO+GUA

As expected^[6], sintering of the NiMo catalyst was observed for t0 experiments. Scherrer law was used to determine Ni⁰ crystallite sizes. At 250°C, used catalysts from BO and BO+GUA conversion, presented respectively an average size of 235 and 203 Å. Between 200 and 300°C (1 h reaction), sintering grew from 175 to 320 Å from BO conversion whereas, it grew from 165 to 250 Å from BO+GUA conversion.

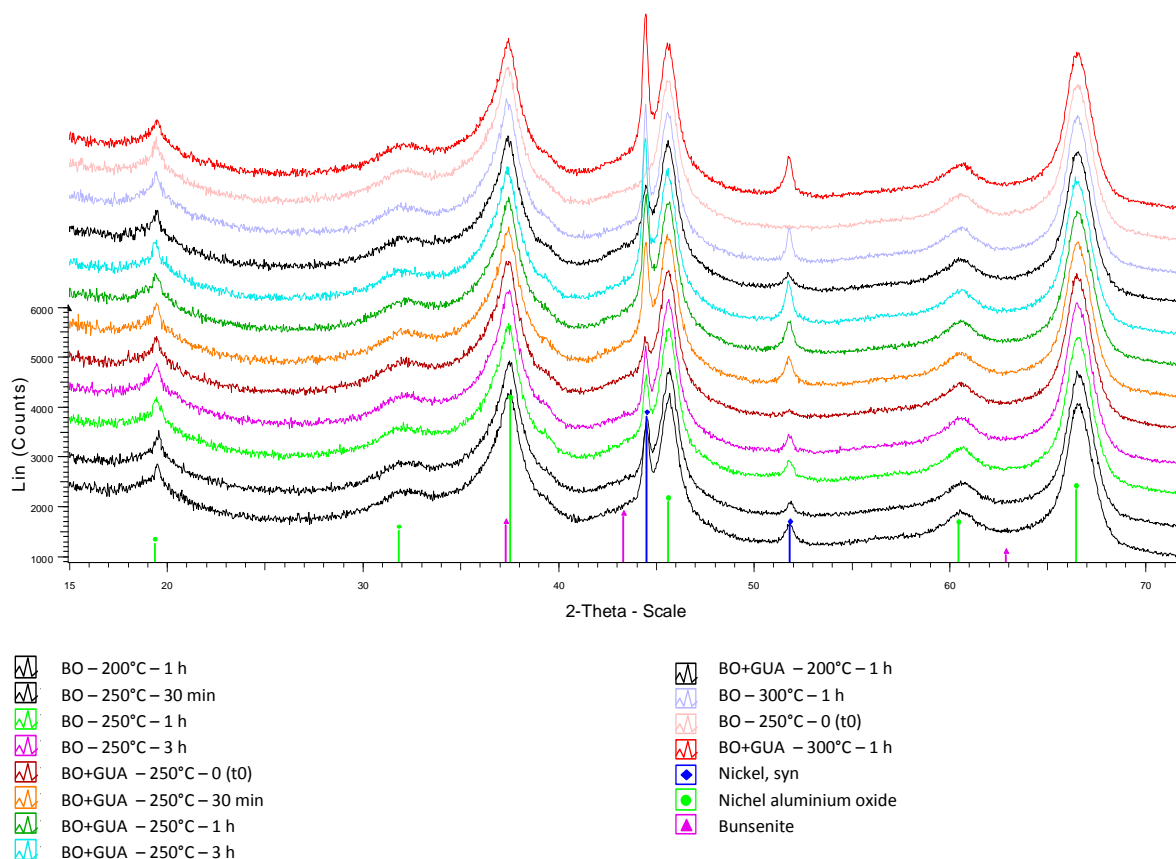


Figure S12. XRD diffractograms of used catalyst the hydroconversion of BO and BO+GUA as a function of time and temperature

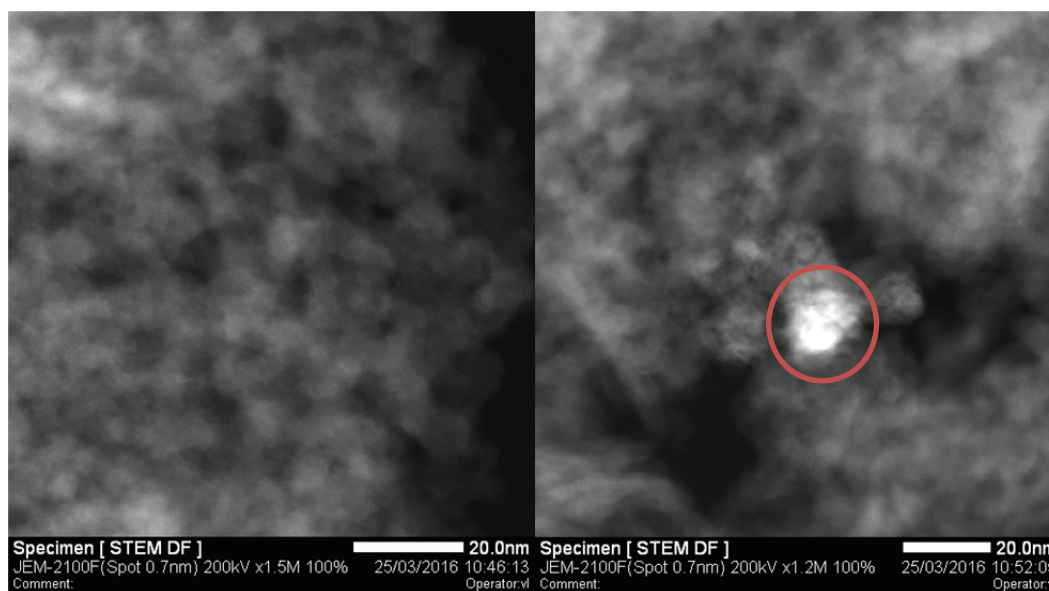
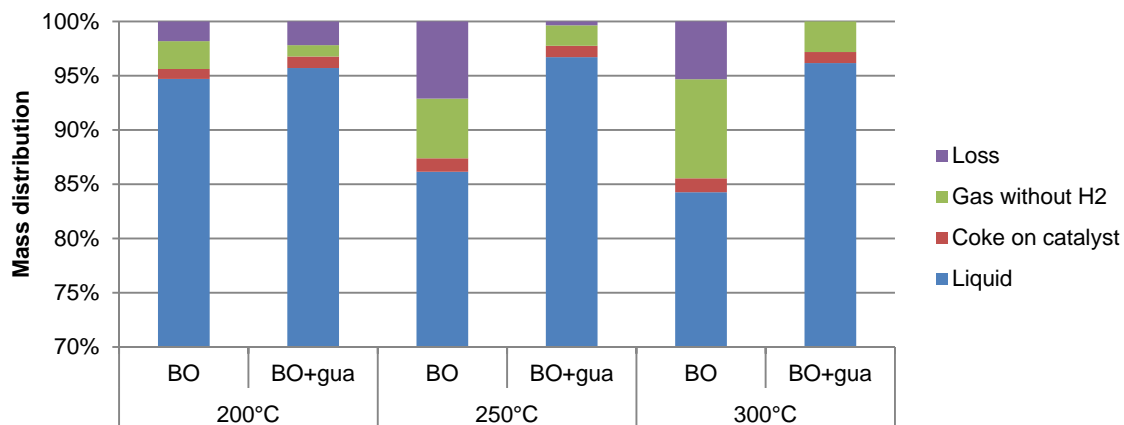


Figure S13. STEM-HAADF pictures of a used catalyst (BO hydroconversion at 200°C – 1h): [A] well dispersed particles, [B] Ni crystallite (red circle)

3.4. Effect of the reaction temperature on the bio-oil and bio-oil/guaiacol catalytic hydroconversion



		200°C		250°C		300°C	
		BO	BO+gua	BO	BO+gua	BO	BO+gua
Mass balance (g)	Liquid	142.6	144.2	129.5	145.6	126.5	144.7
	Coke on catalyst	1.4	1.6	1.9	1.6	1.9	1.5
	Gas without H ₂	3.9	1.6	8.3	2.8	13.7	4.2
	Loss	2.7	3.3	10.7	0.5	8.0	0.0

Figure S14. Mass balances from hydroconverted BO and BO+GUA as a function of temperature (reaction time –1 h)

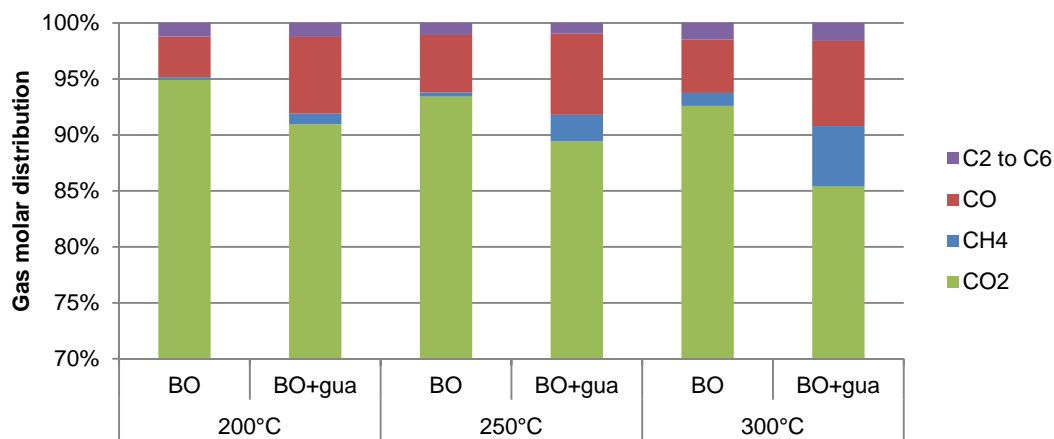


Figure S15. Gas production from hydroconverted BO and BO+GUA as a function of temperature (reaction time –1 h)

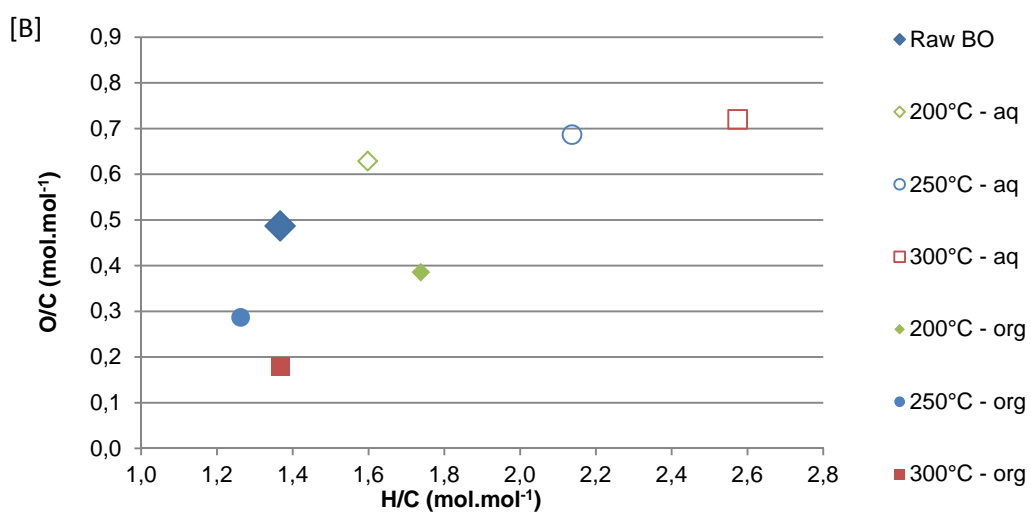
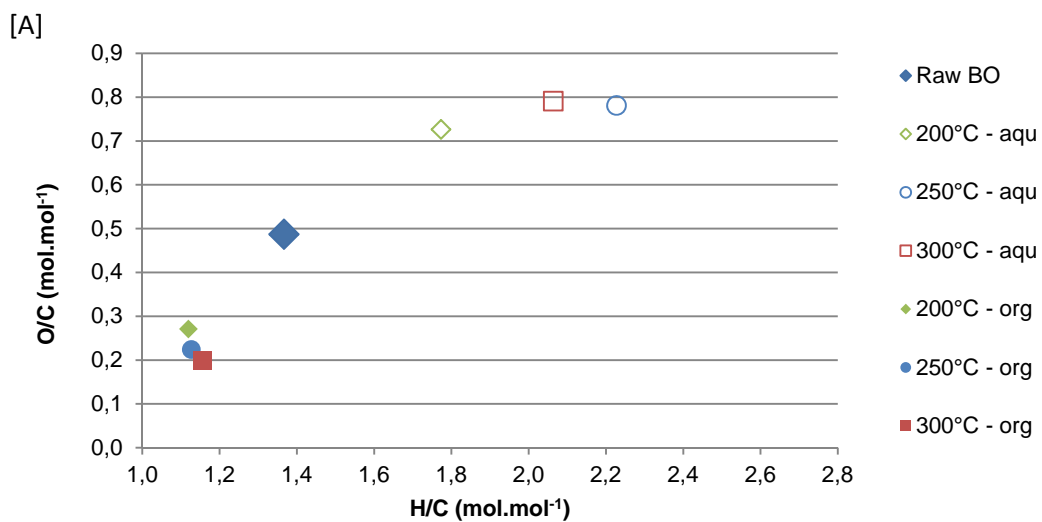


Figure S16. Van Krevelen diagram (Dry basis) reporting the organic and aqueous phases from the hydroconversion of [A] BO and [B] BO+GUA as a function of temperature (reaction time – 1 h). For the mixture, the guaiacol contribution (75 g) was assumed to be exclusively reported in the organic phases.

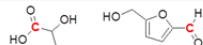
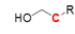
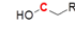

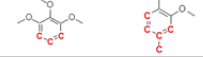

		Bio-oil		Bio-oil + guaiacol	
		Organic	Aqueous	Organic	Aqueous
Carbonyls		↘ ↙	↘ ↙	↔ ↔	↘ ↔
Aliphatic C-C		↘ ↙	↗ ↗	↗ ↗	↗ ↗
Aliphatic C-O		↔ ↘	↔ ↘	↔ ↘	↘ ↘
Aromatic C-O		↘ ↙	↔ ↔	↔ ↗	↔ ↔
Aromatic C-H, C-C		↗ ↗	↔ ↔	↘ ↘	↔ ↗
Methoxy		↔ ↔	↔ ↔	↔ ↔	↔ ↔
Macromolecules		Lignin-like structure ranging up to 8,000 g.mol ⁻¹ PS eq. solubilized into the organic phases : Fast production of macromolecules (aromatic/carbonyl compounds). Increase of the production likely from 300 to 1,000 g.mol ⁻¹ PS eq. aromatic/carbonyl compounds.		Lignin-like structure ranging up to 3,000 g.mol ⁻¹ PS eq. solubilized into the organic phases : Fast production of macromolecules (aromatic/carbonyl compounds). Increase of the production likely from 300 to 1,000 g.mol ⁻¹ PS eq. aromatic/carbonyl compounds.	

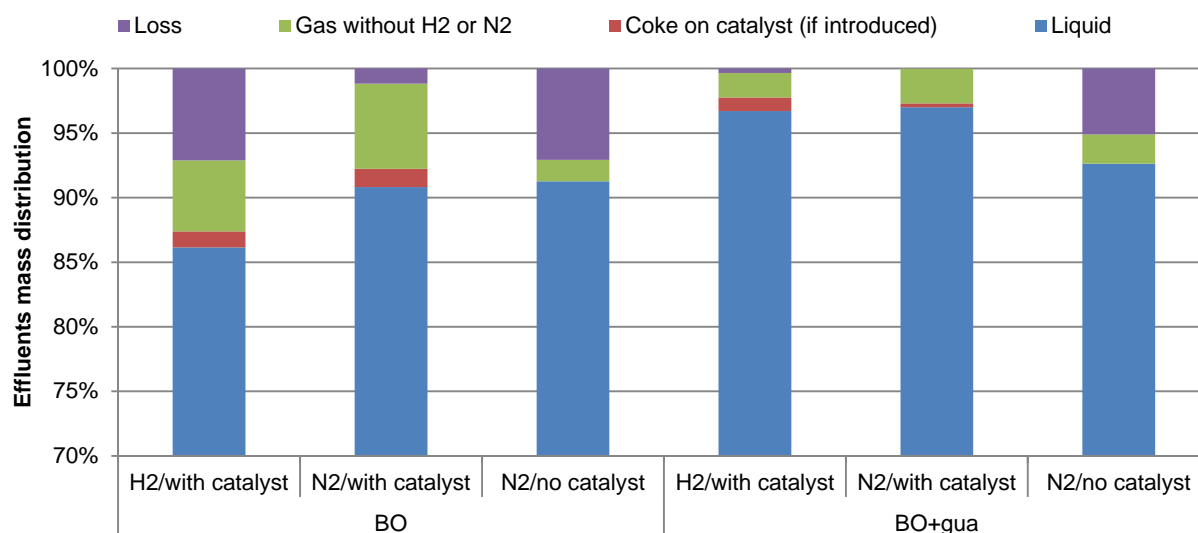
Figure S17. BO and BO+GUA HDC: organic and aqueous phases compositions by ¹³C NMR and macromolecule evolution SEC analysis depending on time (at 250°C from t0 to 3 h in green – left arrows) and temperature (at 1 h from 200 to 300 °C in blue – right arrows)

3.5. Effect of the catalyst and the gas phase composition on the macromolecules production

Considering non-catalytic reactions (investigated in SI, section 3.3.), 30 g of glass beads were introduced (2 mm diameter) representing the same volume than the bulked NiMo catalyst. The reactor was hermetically closed and purged by substituting air by N₂. The initial pressure of nitrogen was set to 3.0 MPa before temperature increase.

We will describe the impact of catalyst presence and gas phase composition added at 250°C during 1 h on the products formed. For both feeds, three operating conditions were screened depending on the gas used (N₂ or H₂ at a total pressure of 13 MPa) and the use of the reduced NiMo/Al₂O₃ catalyst or glass beads (see Experimental section): i) under H₂ with catalyst (referred as H₂/with catalyst), ii) under N₂ with catalyst (referred as N₂/with catalyst) and iii) under N₂ without catalyst (referred as N₂/no catalyst).

For each test, experimental balances (Eq. (1)) and gas phase composition were determined and reported in Fig. S18 to S19.



		BO			BO+gua		
		H2/with catalyst	N2/with catalyst	N2/no catalyst	H2/with catalyst	N2/with catalyst	N2/no catalyst
Mass balance (g)	Liquid	129.5	136.4	133.3	145.6	148.5	145.6
	Coke on catalyst (if introduced)	1.9	2.1	0.0	1.6	0.4	0.0
	Gas without H2 or N2	8.3	9.9	2.4	2.8	4.1	3.6
	Loss	10.7	1.8	10.3	0.5	0.0	8.0

Figure S18. Mass balances from BO and BO+GUA conversion at 250°C during 1 h as a function of the catalyst and the gas phase composition

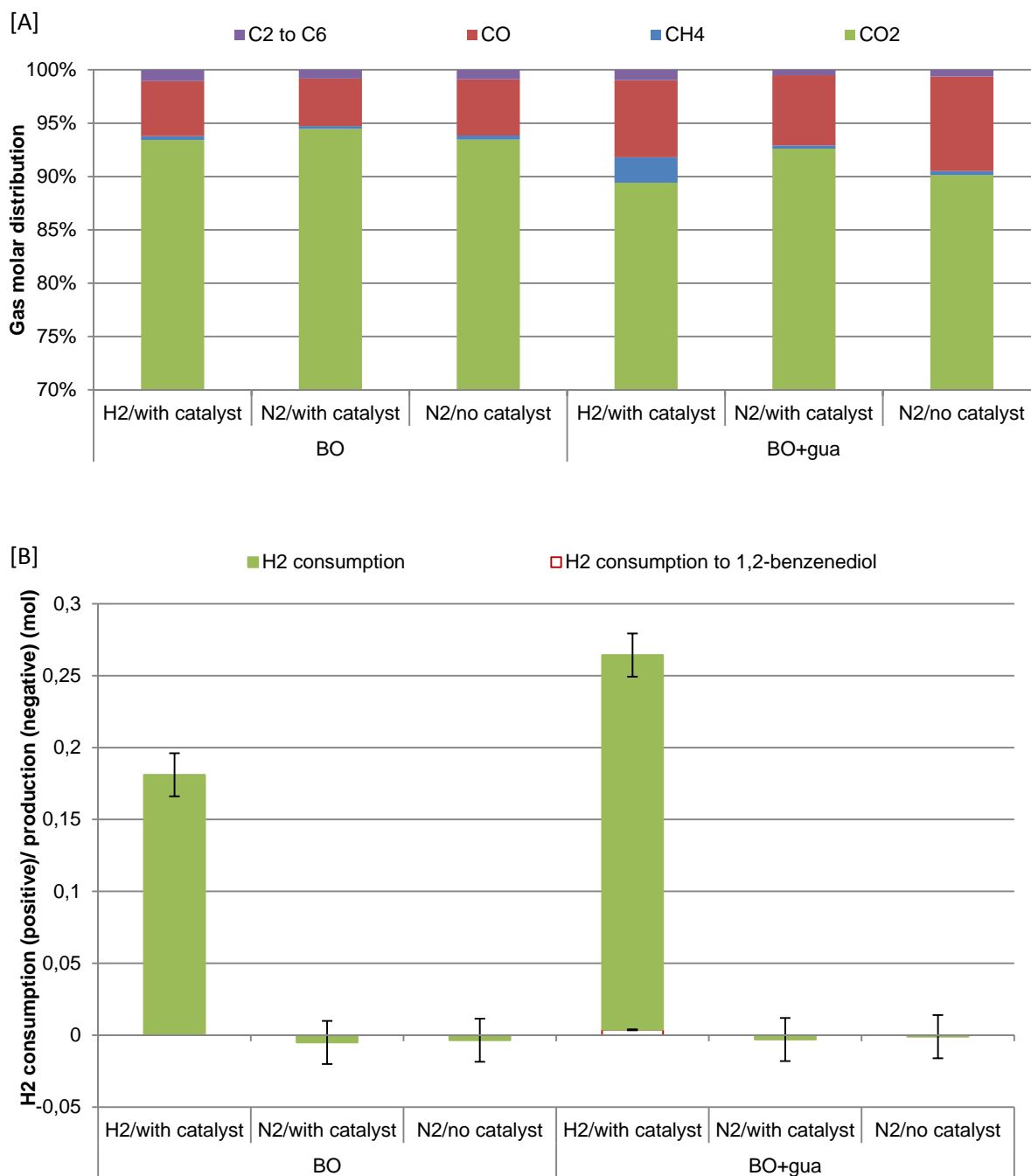


Figure S19. [A] Gas production from BO and BO+GUA conversion at 250°C during 1 h as a function of the catalyst and the gas phase composition. [B] H₂ consumption and production from BO and BO+GUA conversion at 250°C during 1 h as a function of the catalyst and the gas phase composition

No extensive H₂ production (negative value) was observed even for the test “N₂/with catalyst” where reforming and water-gas-shift reactions^[5,6] would be enhanced.

In those operating conditions, no solid were produced except the coke deposited onto the catalyst that will be further investigated. The nature of the gaseous products formed were quite similar for both feed (BO and BO+GUA) and revealed a high content of CO₂ and CO representing at least 90 and 10 mol% respectively.

To assess the macromolecule production, we will consider the liquid phases SEC analysis.

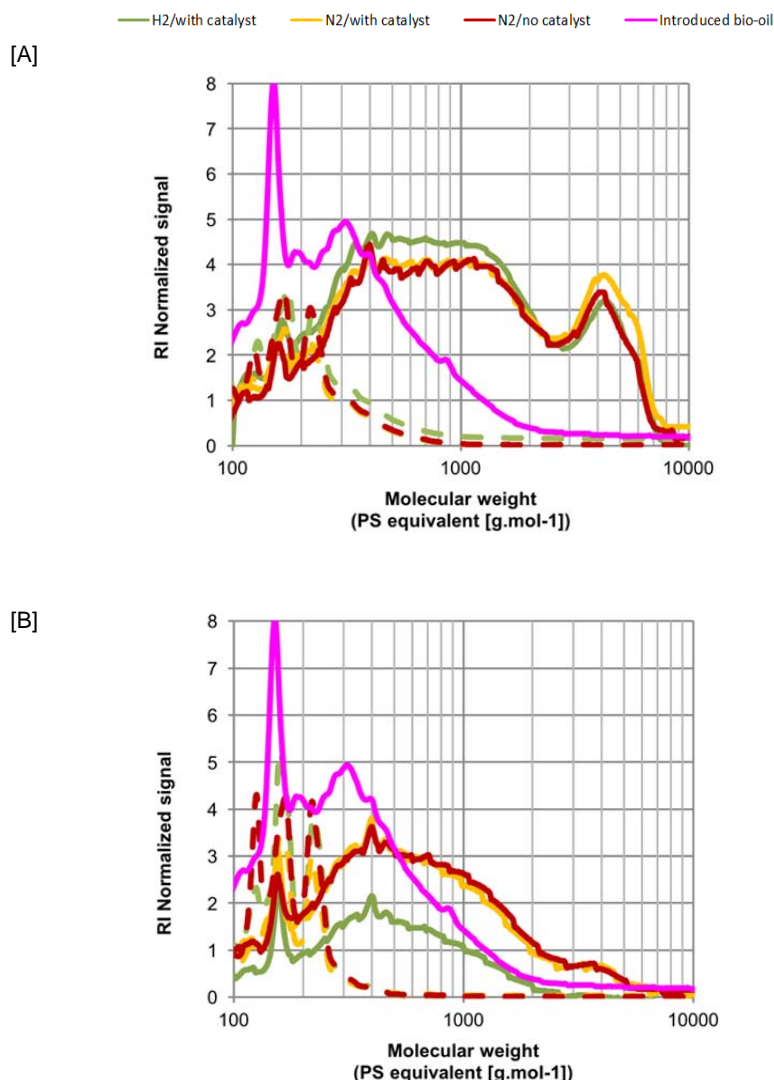


Figure S20. Normalized SEC-RI analyses of converted BO and BO+GUA at 250°C during 1 h from [A] BO, [B] BO+GUA (Continuous lines: organic phase; dotted lines: aqueous phase) as a function of the catalyst and the gas phase composition.

SEC analysis [14, 34] is a tool which enables to characterize macromolecules arising from various biofuels production processes ranging from 100 to 10,000 g.mol⁻¹ in polystyrene equivalent (or PS eq.). SEC-RI analysis reported in Fig. S20 [A] and [B] correspond respectively to the BO and BO+GUA conversion respectively. From BO, macromolecules were produced in the organic phases up to 8,000 g.mol⁻¹ PS eq.. Due to the limit of separation of the used SEC-columns, this value does not indicate the maximum molecular weight. Moreover, because of the detection similitudes, the macromolecule amounts at each molecular mass can be considered as a function of the normalized RI-signals. The production (Fig. S20 [A]) was similar also under N₂ (with or without catalyst) confirming the occurrence of oligomerization/condensation reactions in all operating conditions. Pure guaiacol was calibrated at 85 g.mol⁻¹ PS eq.. Moreover its catalytic hydroconversion in the same operational conditions did not produced compounds greater than 300 g.mol⁻¹ PS eq.[30] Thus SEC profiles correspond to BO conversion. For the three

conditions in presence of guaiacol (Fig. S20 [B]), the size of macromolecules was drastically reduced. To go further in the macromolecules quantification, SEC fractionation was performed on the two organic phases obtained in catalytic hydroconversion conditions (H_2 with catalyst). Resulting mass balances after SEC-solvent evaporation (THF) are reported in Fig. S21 and indicate that 23 wt% of the molecules masses of the converted BO were higher than $1,000 \text{ g.mol}^{-1}$ PS eq. instead of only 3 wt% for the BO+GUA mixture. This result clearly shows that guaiacol help keeping the macromolecule rate to the same level than into the starting BO. For both feeds, aqueous phases did not contain components having a molecular mass higher than $1,000 \text{ g.mol}^{-1}$ PS eq.

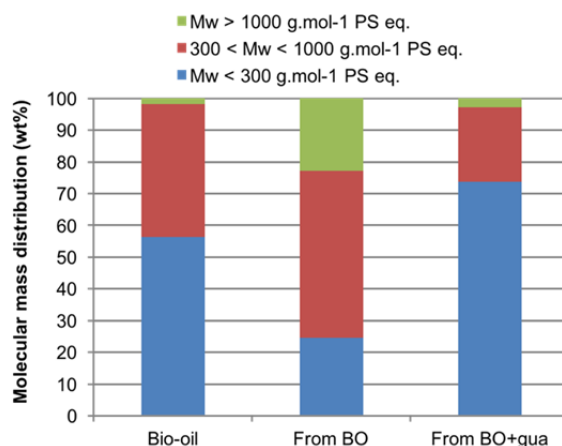


Figure S21. Molecular mass distribution from SEC fractionation of the BO and organic phases from the catalytic hydroconversion of the BO and BO+GUA at 250°C during 1 h.

This is in agreement with the protection of the catalyst textural properties observed in Fig. S22 under N_2 . While used catalyst from the conversion of BO lost 66 % of its initial mesoporous volume (-27 % of its S_{BET}), only 42 % (-12 % of its S_{BET}) were lost during the BO+GUA mixture conversion. In addition, a lower coke deposition was observed with the later feed enhancing the H_2 consumption (Fig. S23).

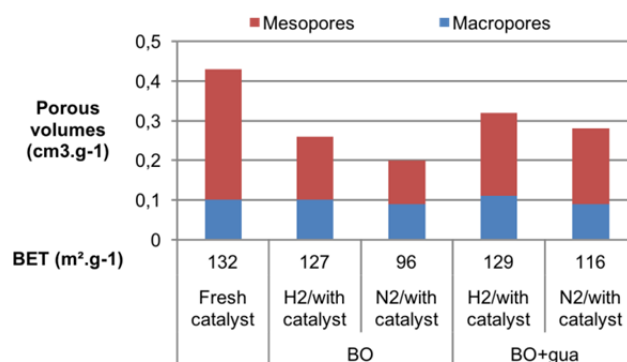


Figure S22. Volumes and BET surfaces of fresh and used catalysts from BO and BO+GUA hydroconversion at 250°C during 1 h as a function of the catalyst and the gas phase composition

To sum up, the NiMo catalyst exhibited a lower activity during the bio-oil conversion due to the massive production of macromolecules (greater than $5,000 \text{ g.mol}^{-1}$ PS eq.). From SEC analysis, these structures were confirmed to arise in homogeneous phase (under N_2 pressure without NiMo catalyst). This production was directly responsible of deep modifications of the catalyst textural properties. The introduction of guaiacol in the feed limited the production of those compounds resulting in a better catalytic activity.

Reaction time	BO				BO+gua			
	0 (t0)	30 min	1 h	3 h	0 (t0)	30 min	1 h	3 h
H ₂ consumption (mmol)	65,8	136,0	181,0	203,0	148,1	230,7	260,6	330,7
H ₂ consumption (mmol/g of BO)	0,44	0,91	1,20	1,35	1,97	3,07	3,47	4,41

Figure S23. H₂ Consumption in mmol and mmol per g of BO

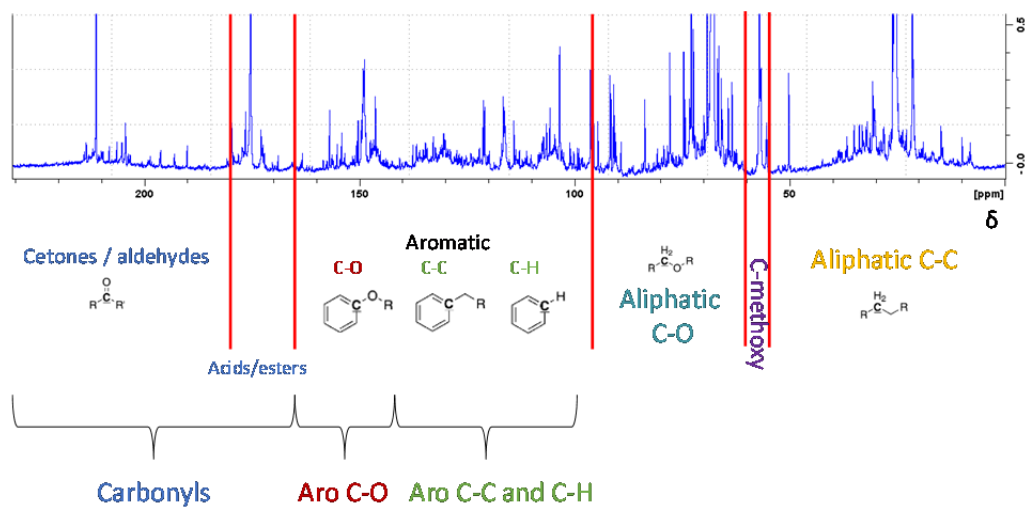


Figure S24. ¹³C NMR spectrum for initial VTT bio-oil

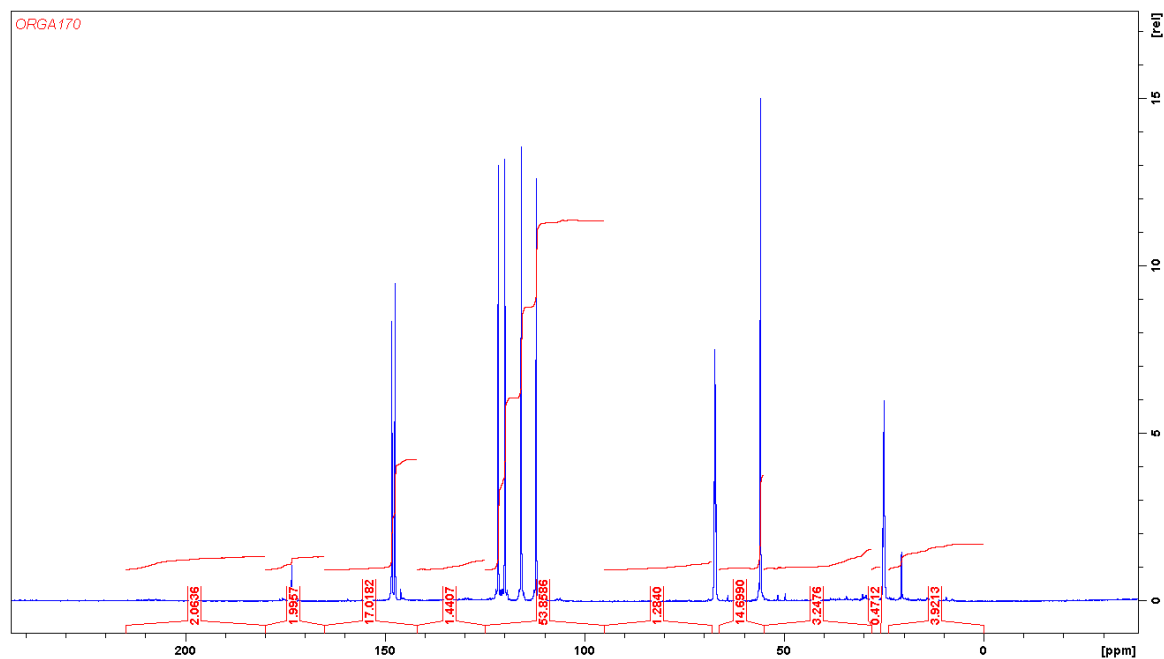


Figure S25. ¹³C NMR spectra of the organic fraction from conversion of (BO+50%GUA) feed

